Proceedings of the 2004 IEEE
International Conference on Control Applications
Taipei, Taiwan, September 2-4, 2004

Using Multi-Frequency for GPS Positioning and Receiver Autonomous Integrity Monitoring

Yi-Hsueh Tsai
Dept. of Electrical Engineering
National Taiwan University
Taipei, Taiwan
d89921013@ntu.edu.tw

Fan-Ren Chang
Dept. of Electrical Engineering
National Taiwan University
Taipei, Taiwan
frchang@cc.ee.ntu.edu.tw

Wen-Chieh Yang
Div. of Research and Development
Intelligent Business Technology Inc.
Taipei, Taiwan
wcyang@ibtek.com.tw

Chia-Lung Ma
Div. of Research and Development
Intelligent Business Technology Inc.
Taipei, Taiwan
mcl@ibtek.com.tw

Abstract: **Algorithms using multi-frequency for GPS positioning and receiver autonomous integrity monitoring (RAIM) are proposed by the authors. In the conventional algorithms, only single frequency L1 is applied. After the L2 and L5 signals are applied, the ionospheric delay can be removed. Therefore, the variance of the measurement error is reduced, the positioning accuracy is improved, and the detection time of satellite failure is decreased. In addition, a cleaner parity vector is obtained, so the incorrect exclusion rate (IER) will be significantly reduced. This paper provides a systematic way to derive the algorithms of the positioning and RAIM for multi-frequency GPS receiver. Simulation results show that, in comparison with the conventional single frequency method, the proposed multi-frequency algorithms not only possess more accurate positioning results, but also demonstrate higher performance in detecting small failures and, in detecting large failures, demonstrate a similar level of performance. Moreover, simulation results also verify that the proposed method has lower IER than the conventional single frequency method has.**

1. Introduction

To improve the performance of the current navigation system, a GPS (global positioning system) modernization policy has been approved by US government. In March 30, 1998, the White House announced that the Block IIR-M GPS satellite carrying L2 signal will be launched in the near future. Furthermore, the Block IIF GPS satellite carrying L2 and L5 signals will be launched in 2005. The main advantages of multi-frequency GPS receiver are performance enhancement in positioning accuracy and receiver autonomous integrity monitoring (RAIM). In addition, the new signal can be regarded as a backup, and thus will significantly increase the safety of navigation [3]. The carrier frequency of L1, L2 and L5 signals [3][10] are 1575.42*M*Hz, 1227.60*M*Hz and 1176.45*M*Hz, respectively. The C/A code in L5 signal is as precise as P code in L1 (or L2).

Conventionally, the algorithms of the positioning and RAIM are based on single frequency only. The purpose of RAIM is to detect the presence of unacceptably large position error and, further, to exclude the error source, thereby allowing the GPS navigation to continue [4]. To achieve this goal, a number of useful algorithms have been published over the last few decades. Parkinson and Axelrad [6] suggested a least-squares residual method for GPS positioning and autonomous satellite failure detection and exclusion. Sturza [8] proposed the standard parity space algorithm to detect the satellite failure and further to exclude the failed one. Pervan [7] used the same algorithm but replaced the code measurement by more accuracy carrier phase measurement.

Algorithms using multi-frequency (L1/L2/L5) for GPS positioning and RAIM are proposed by the authors. The ionospheric delay is highly related to frequency and can be removed by adopting multi-frequency. Therefore, the variance of the measurement error is reduced, the positioning accuracy is improved, and the detection time of satellite failure is decreased. In addition, a cleaner parity vector is obtained, so the incorrect exclusion rate (IER) will be significantly reduced. Simulation results show that, in comparison with the conventional single frequency method, the proposed multi-frequency algorithms not only possess more accurate positioning results, but also demonstrate higher performance in detecting small failures and, in detecting large failures, demonstrate a similar level of performance. Moreover, simulation results also verify that the proposed method has lower IER than the conventional single frequency method has.

The remainders of the paper are organized as follows. Section 2 describes the conventional single frequency algorithms for positioning and RAIM. Section 3 proposes the multi-frequency algorithms for GPS positioning and RAIM. Section 4 verifies the proposed algorithms by conducting simulations. Section 5 concludes this paper.

2. Conventional Single Frequency Algorithms for Positioning and RAIM

The conventional single frequency algorithms for GPS positioning and RAIM are given in this section. Assume the number of the visible satellites is n, and then the GPS measurement equation can be represented as

$$\mathbf{y} = \mathbf{H}\mathbf{x} + \mathbf{e}, \tag{2-1}$$

where $\mathbf{y}$ is the measurement residual vector, $\mathbf{H}$ is the observation matrix, $\mathbf{x}$ is the state vector including the positioning deviation and user clock bias deviation relative to a nominal vector, and $\mathbf{e}$ is a zero mean Gaussian noise vector with covariance matrix $\sigma^2\mathbf{I}_n$ [9][10]. The least-squares estimate of the state vector is

$$\hat{\mathbf{x}}_{LS} = \mathbf{H}^{*}\mathbf{y}, \tag{2-2}$$

where $\mathbf{H}^{*}$ denotes the pseudo inverse of $\mathbf{H}$, and is defined

as $\mathbf{H}^* \equiv (\mathbf{H}^T\mathbf{H})^{-1}\mathbf{H}^T$. Obviously, the positioning accuracy is affected by the value σ^2 of the noise. The least-squares-residual method for fault detection is derived as follows. The estimate of the range is

$$\hat{\mathbf{y}} = \mathbf{H}\hat{\mathbf{x}}_{LS}, \tag{2-3}$$

and the pseudorange residual vector is

$$\mathbf{w} = \mathbf{y} - \hat{\mathbf{y}}. \tag{2-4}$$

By defining the sum of the squares of the range residual errors (SSE) as

$$s \equiv \mathbf{w}^T\mathbf{w}, \tag{2-5}$$

Parkinson and Axelrad [6] showed that the distribution of s/σ^2 is $\chi^2(n-4)$, where $\chi^2(\nu)$ represents the chi-square distribution with ν degrees of freedom. s will be compared with a threshold T_d to judge whether the system is failed or not. The threshold value under a specified false alarm rate can be obtained directly through the cumulative distribution function of $\chi^2(n-4)$.

The parity space method can also perform the fault detection, and more, can exclude the failed satellite. According to [2], there exists a parity matrix $\mathbf{P}$ satisfying the following equation

$$\mathbf{PH} = \mathbf{0} \quad \text{and} \quad \mathbf{PP}^T = \mathbf{I}_{n-4}. \tag{2-6}$$

After the parity matrix $\mathbf{P}$ is found, the parity vector, $\mathbf{p}$, can be defined as

$$\mathbf{p} \equiv \mathbf{Py}. \tag{2-7}$$

Brown [1] showed that

$$\mathbf{p}^T\mathbf{p} = s, \tag{2-8}$$

and thus, as in the least-squares-residual method, the parity space method can also be used to perform the failure detection. In order to maintain sufficient redundancy, at least five visible satellites are required.

After the detection of satellite malfunction, the failed satellite must be excluded to ensure uninterrupted navigation. Given the event of a failure vector $\mathbf{b}$, then (2-1) becomes

$$\mathbf{y} = \mathbf{Hx} + \mathbf{b} + \mathbf{e}. \tag{2-9}$$

Based on the standard parity vector exclusion algorithm [1], the algorithm to identify the failed satellite is as follows

$$n_f = \arg\max_{i=1,\ldots,n} \frac{|\mathbf{p}^T\mathbf{p}_i|}{|\mathbf{p}_i|}, \tag{2-10}$$

where n_f is the channel number of the failed satellite, and $\mathbf{p}_i$ is the i-th column vector of the parity matrix $\mathbf{P}$. $\mathbf{p}_i$ is also called the i-th channel vector since it is related to the i-th satellite. In order to perform the failure exclusion, at least six visible satellites are required. Figure 2-1 gives the plot of a parity space, in which the number of the visible satellites is assumed to be six. In this figure, six channel vectors corresponding to the six visible satellites are shown, and the parity vector is closest to the channel vector associated with the failed satellite. This coincides with the criteria stated in (2-10).

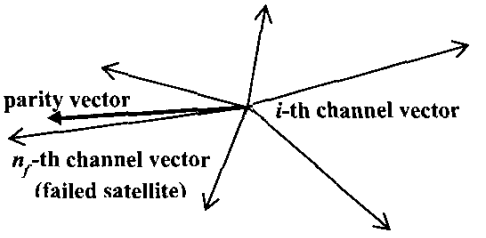

Figure 2-1 Parity space plot with six visible satellites

3. Multi-Frequency GPS Receiver Positioning Algorithms and RAIM

In this section, algorithms based on multi-frequency are proposed to perform the air navigation and receiver autonomous integrity monitoring (RAIM) According to [5], the ionospheric delay can be obtained as follows

$$\text{group delay} = 40.3 f^{-2} TEC_i = f^{-2}\kappa_i, \tag{3-1}$$

where f is the carrier frequency, TEC_i is the total electron content (TEC) in the path where the signal of the i-th satellite go through, κ_i is $40.3TEC$.

3.1. Dual Frequency (L1/L2) Algorithms

The algorithms for dual frequency are given in this subsection. The linearized GPS measurement equations can be expressed as

$$\begin{bmatrix}\mathbf{y}_{L1}\\ \mathbf{y}_{L2}\end{bmatrix} = \begin{bmatrix}\mathbf{H} & f_{L1}^{-2}\mathbf{I}_n\\ \mathbf{H} & f_{L2}^{-2}\mathbf{I}_n\end{bmatrix}\begin{bmatrix}\mathbf{x}\\ \boldsymbol{\kappa}\end{bmatrix} + \begin{bmatrix}\mathbf{e}_{L1}\\ \mathbf{e}_{L2}\end{bmatrix}, \tag{3-2}$$

where $\mathbf{y}_{L1}$ and $\mathbf{y}_{L2}$ are the linearized GPS measurements of L1 and L2, respectively; $\mathbf{x}$ is the positioning deviation and user clock bias deviation relative to a nominal vector; $\boldsymbol{\kappa}$ is defined as $\boldsymbol{\kappa} \equiv [\kappa_1 \cdots \kappa_i \cdots \kappa_n]$, where κ_i is as in (3-1); f_{L1} and f_{L2} are the carrier frequencies for L1 and L2, respectively; $\mathbf{e}_{L1}$ and $\mathbf{e}_{L2}$ are zero mean Gaussian noise vector with covariance matrices $\sigma_{L1}^2\mathbf{I}_n$ and $\sigma_{L2}^2\mathbf{I}_n$, respectively, and are mutually independent. The weighted least squares estimated is

$$\begin{aligned}\begin{bmatrix}\hat{\mathbf{x}}\\ \hat{\boldsymbol{\kappa}}\end{bmatrix} &= \begin{bmatrix}\sigma_{L1}^{-1}\mathbf{H} & \sigma_{L1}^{-1}f_{L1}^{-2}\mathbf{I}_n\\ \sigma_{L2}^{-1}\mathbf{H} & \sigma_{L2}^{-1}f_{L2}^{-2}\mathbf{I}_n\end{bmatrix}^* \begin{bmatrix}\sigma_{L1}^{-1}\mathbf{y}_{L1}\\ \sigma_{L2}^{-1}\mathbf{y}_{L2}\end{bmatrix}\\ &= \begin{bmatrix}\beta^2\delta^{-2}(\mathbf{H}^T\mathbf{H})^{-1} & -\alpha\delta^{-2}\mathbf{H}^*\\ -\alpha\delta^{-2}\mathbf{H}^{*T} & \beta^{-2}(\mathbf{I}_n + \alpha^2\delta^{-2}\mathbf{Q})\end{bmatrix}\\ &\times \begin{bmatrix}\sigma_{L1}^{-1}\mathbf{H}^T & \sigma_{L2}^{-1}\mathbf{H}^T\\ \sigma_{L1}^{-1}f_{L1}^{-2}\mathbf{I}_n & \sigma_{L2}^{-1}f_{L2}^{-2}\mathbf{I}_n\end{bmatrix}\begin{bmatrix}\sigma_{L1}^{-1}\mathbf{y}_{L1}\\ \sigma_{L2}^{-1}\mathbf{y}_{L2}\end{bmatrix},\end{aligned} \tag{3-3}$$

where $\mathbf{H}^* = (\mathbf{H}^T\mathbf{H})^{-1}\mathbf{H}^T$, $\mathbf{Q} = \mathbf{H}(\mathbf{H}^T\mathbf{H})^{-1}\mathbf{H}^T$ and

$$\begin{cases}\alpha = \sigma_{L1}^{-2}f_{L1}^{-2} + \sigma_{L2}^{-2}f_{L2}^{-2}\\ \beta = (\sigma_{L1}^{-2}f_{L1}^{-4} + \sigma_{L2}^{-2}f_{L2}^{-4})^{1/2}\\ \delta = ((\sigma_{L1}^{-2} + \sigma_{L2}^{-2})\beta^2 - \alpha^2)^{1/2} = \sigma_{L1}^{-1}\sigma_{L2}^{-1}|f_{L1}^{-2} - f_{L2}^{-2}|\end{cases}.$$

Then the estimated value is

$$\begin{cases}\hat{\mathbf{x}} = (\mathbf{H}^T\mathbf{H})^{-1}\mathbf{H}^T\mathbf{y}_{L12}\\ \hat{\boldsymbol{\kappa}} = \mathbf{y}_{L12}^{\kappa} - \alpha\beta^{-2}\mathbf{H}\hat{\mathbf{x}}\end{cases}, \tag{3-4}$$

where $\mathbf{y}_{L12} = \left(f_{L2}^{-2} - f_{L1}^{-2}\right)^{-1}\left(f_{L2}^{-2}\mathbf{y}_{L1} - f_{L1}^{-2}\mathbf{y}_{L2}\right)$ and $\mathbf{y}_{L12}^{\kappa} = \beta^{-2}\left(\sigma_{L1}^{-2}f_{L1}^{-2}\mathbf{y}_{L1} + \sigma_{L2}^{-2}f_{L2}^{-2}\mathbf{y}_{L2}\right)$. According to [10], there exists a parity matrix $\mathbf{P}_{DF}$ satisfying the following equation

$$\mathbf{P}_{DF} = \left(\sigma_{L1}^{-2}f_{L1}^{-4} + \sigma_{L2}^{-2}f_{L2}^{-4}\right)^{-1/2}\left[\sigma_{L2}^{-1}f_{L2}^{-2}\mathbf{P} \quad \left(-\sigma_{L1}^{-1}f_{L1}^{-2}\right)\mathbf{P}\right], \tag{3-5}$$

where $\mathbf{P}$ is defined in equation (2-6). After the parity matrix $\mathbf{P}_{DF}$ is found, the parity vector for dual-frequency can be obtained as

$$\mathbf{p}_{DF} = \mathbf{P}_{DF}\begin{bmatrix}\sigma_{L1}^{-1}\mathbf{y}_{L1}\\ \sigma_{L2}^{-1}\mathbf{y}_{L2}\end{bmatrix} = \lambda\mathbf{p}_{L12}, \tag{3-6}$$

where $\lambda = \sigma_{L1}^{-1}\sigma_{L2}^{-1}\left(f_{L1}^{-2} - f_{L2}^{-2}\right)\left(\sigma_{L1}^{-2}f_{L1}^{-4} + \sigma_{L2}^{-2}f_{L2}^{-4}\right)^{-1/2}$ and $\mathbf{p}_{L12} = \mathbf{P}\mathbf{y}_{L12}$. Then, according to (2-8), the test statistic is selected as

$$s_{DF} = \mathbf{p}_{DF}^{T}\mathbf{p}_{DF} = \lambda^2\mathbf{p}_{L12}. \tag{3-7}$$

The distribution of s_{DF} is $\chi^2(n-4)$. The threshold value under a specified false alarm rate can be calculated directly through the cumulative distribution function of $\chi^2(n-4)$.

Represent the column of the parity matrix $\mathbf{P}_{DF}$ as $\mathbf{P}_{DF} = \left[\mathbf{p}_1^{L1} \cdots \mathbf{p}_n^{L1} \ \mathbf{p}_1^{L2} \cdots \mathbf{p}_n^{L2}\right]$. Then the i-th channel vectors for L1 and L2 measurements are

$$\begin{cases}\mathbf{p}_i^{L1} = \left(\sigma_{L1}^{-2}f_{L1}^{-4} + \sigma_{L2}^{-2}f_{L2}^{-4}\right)^{-1/2}\sigma_{L2}^{-1}f_{L2}^{-2}\mathbf{p}_i\\ \mathbf{p}_i^{L2} = -\left(\sigma_{L1}^{-2}f_{L1}^{-4} + \sigma_{L2}^{-2}f_{L2}^{-4}\right)^{-1/2}\sigma_{L1}^{-1}f_{L1}^{-2}\mathbf{p}_i\end{cases}, \tag{3-8}$$

where $\mathbf{p}_i$ is the i-th column vector of the matrix $\mathbf{P}$. According to the standard parity vector exclusion algorithm [1], the satellite failure exclusion algorithm based on the multi-frequency is as follows [9]

$$n_f = \arg\max_{i=1,\ldots,n}\left\{\max\left(\frac{\left|\mathbf{p}_{DF}^{T}\mathbf{p}_i^{L1}\right|}{\left|\mathbf{p}_i^{L1}\right|}, \frac{\left|\mathbf{p}_{DF}^{T}\mathbf{p}_i^{L2}\right|}{\left|\mathbf{p}_i^{L2}\right|}\right)\right\}, \tag{3-9}$$

where n_f is the channel number of the failed satellite. Since $\frac{\left|\mathbf{p}_{DF}^{T}\mathbf{p}_i^{L1}\right|}{\left|\mathbf{p}_i^{L1}\right|} = \frac{\left|\mathbf{p}_{DF}^{T}\mathbf{p}_i\right|}{\left|\mathbf{p}_i\right|} = \frac{\left|\mathbf{p}_{DF}^{T}\mathbf{p}_i^{L2}\right|}{\left|\mathbf{p}_i^{L2}\right|}$, (3-9) can be simplified as

$$n_f = \arg\max_{i=1,\ldots,n}\frac{\left|\mathbf{p}_{DF}^{T}\mathbf{p}_i\right|}{\left|\mathbf{p}_i\right|}. \tag{3-10}$$

where $\mathbf{p}_i$ is the i-th column vector of the matrix $\mathbf{P}$.

3.2. Triple Frequency (L1/L2/L5) Algorithms

The algorithms based on triple frequency GPS receiver are given in this subsection. The linearized triple frequency GPS measurement equations can be expressed as

$$\begin{bmatrix}\mathbf{y}_{L1}\\ \mathbf{y}_{L2}\\ \mathbf{y}_{L5}\end{bmatrix} = \begin{bmatrix}\mathbf{H} & f_{L1}^{-2}\mathbf{I}_n\\ \mathbf{H} & f_{L2}^{-2}\mathbf{I}_n\\ \mathbf{H} & f_{L5}^{-2}\mathbf{I}_n\end{bmatrix}\begin{bmatrix}\mathbf{x}\\ \boldsymbol{\kappa}\end{bmatrix} + \begin{bmatrix}\mathbf{e}_{L1}\\ \mathbf{e}_{L2}\\ \mathbf{e}_{L5}\end{bmatrix}. \tag{3-11}$$

where $\mathbf{y}_{L1}$, $\mathbf{y}_{L2}$ and $\mathbf{y}_{L5}$ are the linearized GPS measurements of L1, L2 and L5, respectively; $\mathbf{x}$ is the positioning deviation and user clock bias deviation relative to a nominal vector; $\boldsymbol{\kappa}$ is defined as $\boldsymbol{\kappa} \equiv \left[\kappa_1 \cdots \kappa_i \cdots \kappa_n\right]$, where κ_i is as in (3-1); f_{L1}, f_{L2} and f_{L5} are the carrier frequencies for L1, L2 and L5, respectively; $\mathbf{e}_{L1}$, $\mathbf{e}_{L2}$ and $\mathbf{e}_{L5}$ are zero mean Gaussian noise vector with covariance matrices $\sigma_{L1}^2\mathbf{I}_n$, $\sigma_{L2}^2\mathbf{I}_n$ and $\sigma_{L5}^2\mathbf{I}_n$, respectively, and are mutually independent. The weighted least squares estimated is

$$\begin{aligned}\begin{bmatrix}\hat{\mathbf{x}}\\ \hat{\boldsymbol{\kappa}}\end{bmatrix} &= \begin{bmatrix}\sigma_{L1}^{-1}\mathbf{H} & \sigma_{L1}^{-1}f_{L1}^{-2}\mathbf{I}_n\\ \sigma_{L2}^{-1}\mathbf{H} & \sigma_{L2}^{-1}f_{L2}^{-2}\mathbf{I}_n\\ \sigma_{L5}^{-1}\mathbf{H} & \sigma_{L5}^{-1}f_{L5}^{-2}\mathbf{I}_n\end{bmatrix}^{*}\begin{bmatrix}\sigma_{L1}^{-1}\mathbf{y}_{L1}\\ \sigma_{L2}^{-1}\mathbf{y}_{L2}\\ \sigma_{L5}^{-1}\mathbf{y}_{L5}\end{bmatrix}\\ &= \begin{bmatrix}\beta^2\delta^{-2}\left(\mathbf{H}^T\mathbf{H}\right)^{-1} & -\alpha\delta^{-2}\mathbf{H}^{*}\\ -\alpha\delta^{-2}\mathbf{H}^{*T} & \beta^{-2}\left(\mathbf{I}_n + \alpha^2\delta^{-2}\mathbf{Q}\right)\end{bmatrix}\\ &\times\begin{bmatrix}\sigma_{L1}^{-1}\mathbf{H}^T & \sigma_{L2}^{-1}\mathbf{H}^T & \sigma_{L5}^{-1}\mathbf{H}^T\\ \sigma_{L1}^{-1}f_{L1}^{-2}\mathbf{I}_n & \sigma_{L2}^{-1}f_{L2}^{-2}\mathbf{I}_n & \sigma_{L5}^{-1}f_{L5}^{-2}\mathbf{I}_n\end{bmatrix}\begin{bmatrix}\sigma_{L1}^{-1}\mathbf{y}_{L1}\\ \sigma_{L2}^{-1}\mathbf{y}_{L2}\\ \sigma_{L5}^{-1}\mathbf{y}_{L5}\end{bmatrix},\end{aligned} \tag{3-12}$$

where $\mathbf{H}^{*} = \left(\mathbf{H}^T\mathbf{H}\right)^{-1}\mathbf{H}^T$, $\mathbf{Q} = \mathbf{H}\left(\mathbf{H}^T\mathbf{H}\right)^{-1}\mathbf{H}^T$, and

$$\begin{cases}\alpha = \sigma_{L1}^{-2}f_{L1}^{-2} + \sigma_{L2}^{-2}f_{L2}^{-2} + \sigma_{L5}^{-2}f_{L5}^{-2}\\ \beta = \left(\sigma_{L1}^{-2}f_{L1}^{-4} + \sigma_{L2}^{-2}f_{L2}^{-4} + \sigma_{L5}^{-2}f_{L5}^{-4}\right)^{1/2}\\ \delta = \left(\left(\sigma_{L1}^{-2} + \sigma_{L2}^{-2} + \sigma_{L5}^{-2}\right)\beta^2 - \alpha^2\right)^{1/2}\end{cases}.$$

Then the estimated value is

$$\begin{cases}\hat{\mathbf{x}} = \left(\mathbf{H}^T\mathbf{H}\right)^{-1}\mathbf{H}^T\mathbf{y}_{L125}\\ \hat{\boldsymbol{\kappa}} = \mathbf{y}_{L125}^{\kappa} - \alpha\beta^{-2}\mathbf{H}\hat{\mathbf{x}}\end{cases}, \tag{3-13}$$

where $\mathbf{y}_{L125}^{\kappa} = \beta^{-2}\left(\sigma_{L1}^{-2}f_{L1}^{-2}\mathbf{y}_{L1} + \sigma_{L2}^{-2}f_{L2}^{-2}\mathbf{y}_{L2} + \sigma_{L5}^{-2}f_{L5}^{-2}\mathbf{y}_{L5}\right)$, $\mathbf{y}_{L125} = c_{L1}\mathbf{y}_{L1} + c_{L2}\mathbf{y}_{L2} + c_{L5}\mathbf{y}_{L5}$, and

$$\begin{cases}c_{L1} = \sigma_{L1}^{-2}\delta^{-2}\left(\beta^2 - \alpha f_{L1}^{-2}\right)\\ c_{L2} = \sigma_{L2}^{-2}\delta^{-2}\left(\beta^2 - \alpha f_{L2}^{-2}\right)\\ c_{L5} = \sigma_{L5}^{-2}\delta^{-2}\left(\beta^2 - \alpha f_{L5}^{-2}\right)\end{cases}.$$

According to [10], there exists a parity matrix $\mathbf{P}_{TF}$ satisfying the following equation

$$\mathbf{P}_{TF} = \delta\beta^{-1}\begin{bmatrix}\sigma_{L1}c_{L1}\mathbf{P} & \sigma_{L2}c_{L2}\mathbf{P} & \sigma_{L5}c_{L5}\mathbf{P}\\ \sigma_{L1}d_{L1}\mathbf{I}_n & \sigma_{L2}d_{L2}\mathbf{I}_n & \sigma_{L5}d_{L5}\mathbf{I}_n\end{bmatrix}, \tag{3-14}$$

where $\mathbf{P}$ is defined in equation (2-6) and

$$\begin{cases}d_{L1} = \delta^{-2}\beta\sigma_{L1}^{-1}\sigma_{L2}^{-1}\sigma_{L5}^{-1}\left(f_{L2}^{-2} - f_{L5}^{-2}\right)\\ d_{L2} = \delta^{-2}\beta\sigma_{L1}^{-1}\sigma_{L2}^{-1}\sigma_{L5}^{-1}\left(f_{L5}^{-2} - f_{L1}^{-2}\right)\\ d_{L5} = \delta^{-2}\beta\sigma_{L1}^{-1}\sigma_{L2}^{-1}\sigma_{L5}^{-1}\left(f_{L1}^{-2} - f_{L2}^{-2}\right)\end{cases}.$$

After the parity matrix $\mathbf{P}_{TF}$ is found, the parity vector for triple frequency can be obtained as

$$\mathbf{p}_{TF} = \mathbf{P}_{TF}\begin{bmatrix}\sigma_{L1}^{-1}\mathbf{y}_{L1}\\ \sigma_{L2}^{-1}\mathbf{y}_{L2}\\ \sigma_{L5}^{-1}\mathbf{y}_{L5}\end{bmatrix} = \delta\beta^{-1}\begin{bmatrix}\mathbf{p}_{L125}\\ \mathbf{z}_{L125}\end{bmatrix}, \tag{3-15}$$

where $\mathbf{z}_{L125} = d_{L1}\mathbf{y}_{L1} + d_{L2}\mathbf{y}_{L2} + d_{L5}\mathbf{y}_{L5}$ and $\mathbf{p}_{L125} = \mathbf{P}\mathbf{y}_{L125}$. Then, according to (2-8), the test statistic is selected as

$$s_{TF} = \mathbf{p}_{TF}^{T}\mathbf{p}_{TF} = \delta^2\beta^{-2}\left(\mathbf{p}_{L125}^{T}\mathbf{p}_{L125} + \mathbf{z}_{L125}^{T}\mathbf{z}_{L125}\right). \tag{3-16}$$

The distribution of s_{TF} is $\chi^2(n-4)$. The threshold value under a specified false alarm rate can be calculated directly through the cumulative distribution function of $\chi^2(n-4)$.

Represent the column of the parity matrix $\mathbf{P}_{TF}$ as

$$\mathbf{P}_{TF} = \left[\mathbf{p}_1^{L1} \cdots \mathbf{p}_n^{L1}\ \mathbf{p}_1^{L2} \cdots \mathbf{p}_n^{L2}\ \mathbf{p}_1^{L5} \cdots \mathbf{p}_n^{L5}\right], \quad (3\text{-}17)$$

then the i-th channel vectors for L1, L2, and L5 measurements are

$$\begin{cases} \mathbf{p}_i^{L1} = \delta\beta^{-1}\begin{bmatrix} \sigma_{L1}c_{L1}\mathbf{p}_i \\ \sigma_{L1}d_{L1}\mathbf{u}_i \end{bmatrix} \\ \mathbf{p}_i^{L2} = \delta\beta^{-1}\begin{bmatrix} \sigma_{L2}c_{L2}\mathbf{p}_i \\ \sigma_{L2}d_{L2}\mathbf{u}_i \end{bmatrix} \\ \mathbf{p}_i^{L5} = \delta\beta^{-1}\begin{bmatrix} \sigma_{L5}c_{L5}\mathbf{p}_i \\ \sigma_{L5}d_{L5}\mathbf{u}_i \end{bmatrix} \end{cases}, \quad (3\text{-}18)$$

where $\mathbf{p}_i$ is the i-th column vector of the matrix $\mathbf{P}$, $\mathbf{u}_i$ is the unit vector with all elements zeros except the i-th element is one. According to the standard parity vector exclusion algorithm [1], the satellite failure exclusion algorithm based on the triple frequency is as follows [9]

$$n_f = \arg\max_{i=1,\ldots,n}\left\{\max\left(\frac{\left|\mathbf{p}_{TF}^T\mathbf{p}_i^{L1}\right|}{\left|\mathbf{p}_i^{L1}\right|}, \frac{\left|\mathbf{p}_{TF}^T\mathbf{p}_i^{L2}\right|}{\left|\mathbf{p}_i^{L2}\right|}, \frac{\left|\mathbf{p}_{TF}^T\mathbf{p}_i^{L5}\right|}{\left|\mathbf{p}_i^{L5}\right|}\right)\right\}, \quad (3\text{-}19)$$

where n_f is the channel number of the failed satellite.

4. Simulation and Analysis

Monte Carlo simulations are conducted to verify the proposed algorithms. The software package "Satellite Navigation TOOLBOX for Matlab" by GPSoft LLC is adopted in the simulation. It assumed a 24-satellite constellation with perfectly circular orbits. The thermal noise, tropospheric delay, and ionospheric delay are added to the pseudoranges of all satellites. In addition, the receiver mask angle is set as 7.5°.

4.1. Positioning

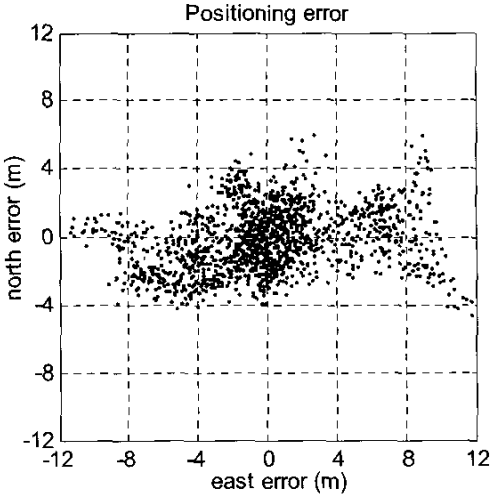

(a) Single frequency

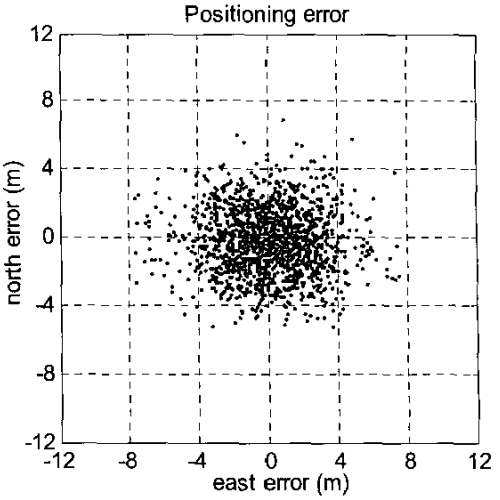

(b) Dual frequency

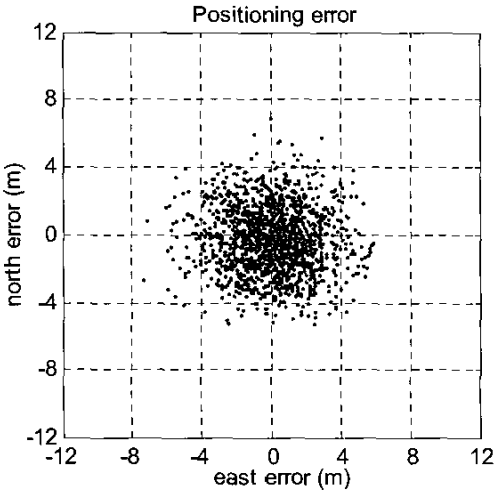

(c) Triple frequency

Figure 4-1 Positioning error

To verify that the proposed algorithm can improve the positioning performance, a total of 1440 sample points were produced. The simulation time is every minute for 24 hours starting at midnight at the beginning of the GPS week, and the location is selected at the latitude 0°N and longitude 0°E. The simulation results of the positioning are plotted in Figure 4-1(a), Figure 4-1(b) and Figure 4-1(c), respectively. It can be seen that, in comparison with the conventional single frequency method, the proposed multi-frequency algorithms possess more accurate positioning results. The positioning error of multi-frequency is more concentrated around the origin due to the reduction of measurement error since the ionospheric delay is removed by adopting multi-frequency.

4.2. Satellite Failure Detection

To verify that the proposed algorithm can reduce the

detection time, both ramp-type and step-type failures are used to simulate satellite malfunction. A total of 1152 (24×48) space-time sample points were produced according to the user locations and simulation times mentioned in [11]. The user locations covering the 24 geographic locations are listed in Table 4-1, and the simulation time is every half hour for 24 hours starting at midnight at the beginning of the GPS week. A detection time (DT) can be obtained for each point. DT is defined as the time needed from the onset of the failure to the annunciation of an alarm signal. The average detection time (ADT) is the sample mean of the 1152 values of the DT.

Table 4-1 Geographic locations for simulation

Name	Latitude	Longitude
London	52°N	0°W
Liberia	7°N	10°W
South Atlantic	30°S	15°W
Iceland	65°N	22°W
St. Johns	49°N	52°W
Buenos Aires	30°S	58°W
Ecuador	3°S	80°W
New Orleans	30°N	90°W
Winnipeg	50°N	95°W
Easter Island	27°S	112°W
Los Angeles	34°N	118°W
Central Pacific	5°S	135°W
North Alaska	70°N	150°W
Honolulu	22°N	158°W
Ross Sea	75°S	180°W
New Zealand	40°S	175°E
Marshall Islands	8°N	170°E
Tokyo	36°N	140°E
Perth	32°S	115°E
Singapore	2°N	104°E
Indian Ocean	45°S	75°E
Aral Sea	45°N	60°E
Madagascar	15°S	50°E
Cape Town	35°S	18°E

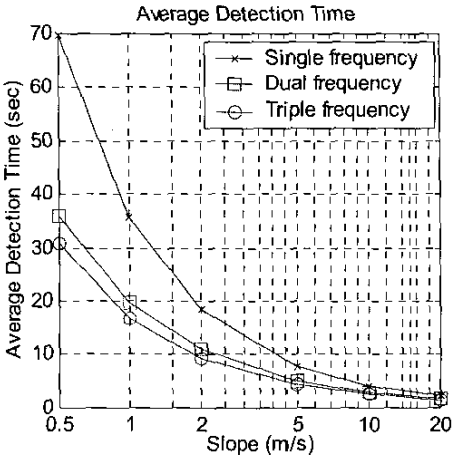

Figure 4-2 ADT for ramp-type failure

The simulation result of ADT for ramp-type failure is plotted in Figure 4-2. The value of slope ranges from 0.5 to 20m/s. The percentage of improvement can be obtained through the following equation

$$\frac{ADT(SF)-ADT(MF)}{ADT(SF)}\times 100\%, \qquad (4\text{-}1)$$

where ADT(SF) is the ADT when the single frequency (L1) is applied, ADT(MF) is the ADT when the multi-frequency (dual frequency or triple frequency) is applied. The best improvement percentage for dual frequency and triple frequency are 48.3% and 55.9%, respectively.

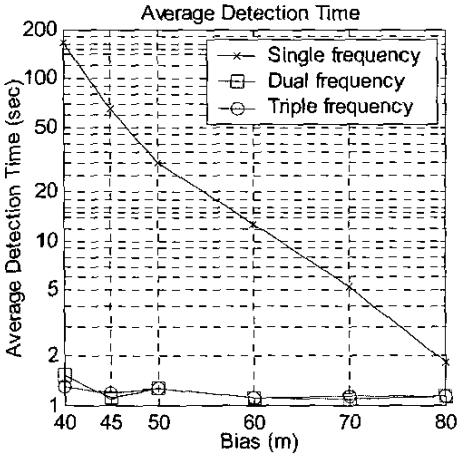

(a) Single frequency v.s. multi-frequency

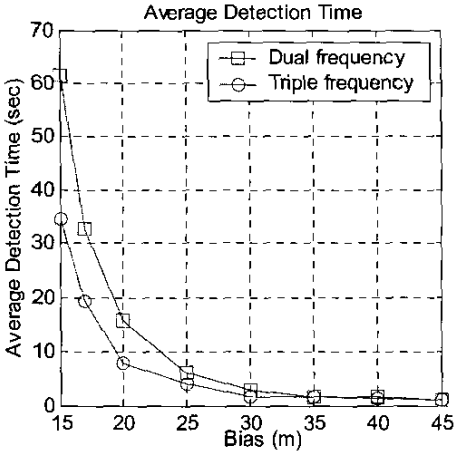

(b) Dual frequency v.s. Triple frequency

Figure 4-3 ADT for step-type failure

The simulation result of ADT for step-type pseudo-range failure is plotted in Figure 4-3(a) and (b), respectively. The value of bias ranges from 15 to 80m. The percentage of improvement can be obtained through (4-1). The best improvement percentage for dual frequency and triple frequency are 99.1% and 99.2%, respectively. Simulation results show that, in comparison with the conventional single frequency method, the triple-frequency algorithms demonstrates higher performance in detecting small

failures and, in detecting large failures, demonstrates a similar level of performance.

4.3. Satellite Failure Detection

To show that the proposed algorithm can reduce the incorrect exclusion rate, the step-type failure is used to simulate satellite malfunction. The value of bias ranges from 15 to 50m. In order to evaluate the performance of the proposed algorithm, the concept of incorrect exclusion (IE) is introduced. An IE occurs when the receiver performs a valid detection, but the failed satellite remains in the solution after the exclusion operation [4]. The incorrect exclusion rate (IER), which is used as a performance index, is defined as

$$IER = \frac{\text{no. of incorrect exclusion}}{\text{no. of total exclusion}} \times 100\% . \qquad (4\text{-}2)$$

IER can be used to verify the superior exclusion capability of the proposed algorithms. Simulation results are plotted in Figure 4-4. Simulation results show that the IER obtained through the dual frequency is lower than the one through the conventional single frequency, and the IER obtained through the triple frequency is lower than the one through the dual frequency. In conclusion, simulation results verify that the proposed method has lower IER than the conventional single frequency method has.

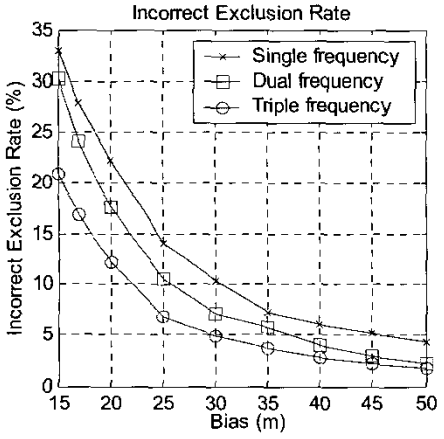

Figure 4-4 Incorrect exclusion rate

5. Conclusion

Algorithms using multi-frequency (L1/L2/L5) for GPS positioning and RAIM are proposed by the authors. In the conventional algorithms, only single frequency L1 is applied. After the L2 and L5 signals are adopted, the ionospheric delay can be removed. Therefore, the variance of the measurement error is reduced, the positioning accuracy is improved, and the detection time of satellite failure is decreased. In addition, a cleaner parity vector is obtained, so the incorrect exclusion rate (IER) will be significantly reduced. Simulation results show that, in comparison with the conventional single frequency method, the proposed multi-frequency algorithms possess more accurate positioning results. The positioning error of multi-frequency is more concentrated around the origin due to the reduction of measurement error. The simulation results of ramp-type failure detection show that the best improvement percentage for dual frequency and triple frequency are 48.3% and 55.9%, respectively. As for the case of step-type failure detection, the best improvement percentage for dual frequency and triple frequency are 99.1% and 99.2%, respectively. Moreover, the incorrect exclusion rate (IER) obtained through the dual frequency is lower than the one through the conventional single frequency, and the IER obtained through the triple frequency is lower than the one through the dual frequency.

References

[1] Brown, R. G., "A Baseline GPS RAIM Scheme and a Note on the Equivalence of Three RAIM Methods," *Navigation, Journal of the Institute of Navigation*, Vol. 39, No.3, 1992, pp. 301-316.

[2] Diggelen, V. F. and Brown, A., "Mathematical Aspects of GPS RAIM," *Position Location and Navigation Symposium, IEEE*, 1994, pp.733-738.

[3] Fontana, D. R., Cheung, W., and Stansell T., "The Modernized L2 Civil Signal: Leaping Forward in the 21st Century," *GPS World*, September, 2001, pp.28-34. (http://www.gpsworld.com)

[4] Lee, Y, Dyke K. V., Decleene B., Studenny J., and Beckmann M., "Summary of RTCA SC-159 GPS Integrity Working Group Activities," *Navigation, Journal of the Institute of Navigation*, Vol. 43, No.3, 1996.

[5] Misra, P., and Enge, P., "Global Positioning System: Signals, Measurements, and Performance," Ganga-Jamuna Press, 2001

[6] Parkinson, B. W. and Axelrad, P., "Autonomous GPS Integrity Monitoring Using the Pseudorange Residual," *Navigation, Journal of the Institute of Navigation*, Vol. 35, No.2, 1988, pp. 255-274.

[7] Pervan, B. S., et. al, "Parity Space Method for Autonomous Fault Detection and Exclusion Algorithm Using Carrier Phase," *Position Location and Navigation Symposium, IEEE*, 1996, pp. 649-656.

[8] Sturza, M. A., "Navigation System Integrity Monitoring Using Redundant Measurements", *Navigation, Journal of the Institute of Navigation*, Vol. 35, No.4, 1988, pp.483-501.

[9] Tsai, Y. H., Chang, F. R., and Yang, W. C., "Moving Average Filters for Faster GPS Receiver Autonomous Integrity Monitoring," *2002 ION National Technical Meeting*, 2002, pp. 666-675.

[10] Tsai, Y. H., Chang, F. R., Yang, W. C., and Wang, H. S., "Multi-Frequency (L1/L2/L5) Algorithms for Satellite Failure Isolation," *The ION 58th Annual Meeting and the CIGTF 21st Guidance Test Symposium*, 2002, pp. 250~260.

[11] *Minimum Operational Performance Standards for Airborne Supplemental Navigation Equipment Using Global Positioning System (GPS).* Document RTCA/DO-208, Radio Technical Commission for Aeronautics, 1991.